PHYSICAL REVIEW D **87,** 074508 (2013)

Thermal QCD transition with two flavors of twisted mass fermions

Florian Burger,[1] Ernst-Michael Ilgenfritz,[1,2] Malik Kirchner,[1] Maria Paola Lombardo,[3] Michael Müller-Preussker,[1] Owe Philipsen,[4] Christopher Pinke,[4] Carsten Urbach,[5] and Lars Zeidlewicz[4]

(tmfT Collaboration)

[1]*Humboldt-Universität zu Berlin, Institut für Physik, 12489 Berlin, Germany*
[2]*Joint Institute for Nuclear Research, VBLHEP, 141980 Dubna, Russia*
[3]*Laboratori Nazionali di Frascati, INFN, 100044 Frascati, Rome, Italy*
[4]*Goethe-Universität Frankfurt, Institut für Theoretische Physik, 60438 Frankfurt am Main, Germany*
[5]*Universität Bonn, HISKP and Bethe Center for Theoretical Physics, 53115 Bonn, Germany*
(Received 18 February 2013; published 30 April 2013)

We investigate the thermal QCD transition with two flavors of maximally twisted mass fermions for a set of pion masses, 300 MeV $< m_\pi <$ 500 MeV, and lattice spacings, $a < 0.09$ fm. We determine the pseudocritical temperatures and discuss their extrapolation to the chiral limit using scaling forms for different universality classes, as well as the scaling form for the magnetic equation of state. For all pion masses considered, we find reasonable consistency with $O(4)$ scaling plus leading corrections. However, a true distinction between the $O(4)$ scenario and a first-order scenario in the chiral limit requires lighter pions than are currently in use in simulations of Wilson fermions.

DOI: 10.1103/PhysRevD.87.074508 PACS numbers: 11.15.Ha, 11.10.Wx, 11.30.Rd, 12.38.Gc

I. INTRODUCTION

The transition from a confined phase with broken chiral symmetry to a deconfined chirally symmetric phase is an important subject for studies of finite temperature QCD. This transition is relevant for the evolution of the early Universe and reproduced in current heavy ion collision experiments. It can be investigated nonperturbatively using lattice QCD as long as the chemical potential for fermion number is small, $\mu/T < 1$. A lot of effort has been invested in lattice studies at zero chemical potential; for recent reviews, see Refs. [1–4]. Impressive progress has been reported very recently by several collaborations working with different fermion discretization schemes [5–10]. In particular, lattice QCD with staggered fermions and physical quark masses does not predict a true phase transition but an analytic crossover in the limit of zero chemical potential [11]. Similarly, results on the transition temperature and the equation of state have predominantly been obtained from simulations with staggered fermions [12–16]. However, this fermion discretization is subject to an ongoing debate, and there is no formal proof that its continuum limit will reproduce the universality class of QCD [17]. It is therefore desirable to obtain independent results with other discretizations, in order to have some mutual control over systematic errors.

Unfortunately, Wilson-type fermions (and even more so chiral fermion formulations) require higher computational costs. It is thus expedient to study the nature of the phase transition for various larger-than-physical quark masses and to extrapolate to the physical situation. Moreover, knowing global properties of the phase transition as a function of the light quark masses constrains the enlarged phase diagram including the strange quark and nonvanishing chemical potential [18]. An as yet unsettled crucial question in this context is the nature of the phase transition in the two-flavor chiral limit. Most studies favor a second-order transition in the $O(4)$ universality class [19–24], but there are also claims for a first-order transition [25–29]. Since in the continuum and chiral limits the transition is associated with the breaking of a global chiral symmetry, it is necessarily a true and nonanalytic phase transition, and one of these scenarios has to be realized [30], while an analytic crossover is ruled out. On the other hand, for moderate and intermediate quark masses, the transition is an analytic crossover before it turns into a first-order deconfinement transition for very heavy quarks.

In this article we study the thermal transition with two degenerate flavors of maximally twisted mass fermions, which provide an $\mathcal{O}(a)$-improved Wilson fermion discretization; for a review, see Ref. [31]. As a first step, we focus on the determination of the phase boundary, i.e., the pseudocritical temperatures $T_c(m_\pi)$ using the Polyakov loop, the chiral condensate, and the plaquette as observables. We do this for a set of pion masses, $m_\pi \approx$ 300–500 MeV, and attempt various extrapolations to the $N_f = 2$ chiral limit. Similar efforts were recently under way employing clover improved fermions [32–34].

The following section serves to specify our simulation setup. In Sec. III we introduce the observables and collect the pseudocritical couplings from our simulations. These results allow also for an estimate of the size of the discretization errors present in our simulations. In Sec. IV we use these pseudocritical points for an extrapolation to the chiral limit. We discuss possibilities and limitations in discerning the order of the chiral phase transition. Finally, Sec. V gives some conclusions and an outlook.

II. SIMULATION SETUP

We consider QCD with a mass-degenerate doublet of twisted mass fermions, cf. the review by Shindler [31]. The gauge action is tree-level Symanzik improved, while the fermion action is

$$S_F[U,\psi,\bar{\psi}] = \sum_x \bar{\chi}(x)(1-\kappa D_W[U] + 2\mathrm{i}\kappa a\mu_0\gamma_5\tau^3)\chi(x). \tag{1}$$

The fermion fields are written in the twisted basis $\{\bar{\chi},\chi\}$, which is commonly used for numerical simulations. It is connected to the basis of physical fields $\{\bar{\psi},\psi\}$ for the relevant case of maximal twist via

$$\psi = \frac{1}{\sqrt{2}}(1+\mathrm{i}\gamma_5\tau^3)\chi \quad \text{and} \quad \bar{\psi} = \bar{\chi}\frac{1}{\sqrt{2}}(1+\mathrm{i}\gamma_5\tau^3). \tag{2}$$

The quark mass is determined by the hopping parameter κ, which parameterizes the untwisted bare quark mass component,

$$\kappa = (2am_0 + 8r)^{-1}, \tag{3}$$

and the twisted mass parameter μ_0. The Wilson covariant derivative is given by

$$D_W[U]\psi(x) = \sum_\mu((r-\gamma_\mu)U_\mu(x)\psi(x+\hat{\mu}) + (r+\gamma_\mu)U_\mu^\dagger(x-\hat{\mu})\psi(x-\hat{\mu})). \tag{4}$$

In the weak coupling limit, $\beta = 6/g_0^2 \to \infty$, zero quark mass corresponds to $\kappa = 1/8$, setting $r=1$. For finite coupling, this value of κ gets corrections through mass renormalization. The overall renormalized quark mass M is composed of the twisted and untwisted masses as

$$M^2 = Z_m^2(m_0 - m_{\mathrm{cr}})^2 + Z_\mu^2\mu_0^2. \tag{5}$$

At maximal twist, the above fermion formulation is automatically $\mathcal{O}(a)$-improved, i.e., cutoff effects linear in the lattice spacing a are absent for nonzero physical observables. Maximal twist is achieved by tuning the hopping parameter to its critical value κ_c, corresponding to m_{cr}, where the untwisted theory would feature massless pions. The required knowledge of $\kappa_c(\beta)$, as well as other input needed from zero-temperature simulations in order to set the scale, can be interpolated from data by the European Twisted Mass Collaboration (ETMC) [35]. In Figs. 1 and 2, we show our interpolations for $\kappa_c(\beta)$ and the lattice spacing $a(\beta)$. Our numerical evaluation proceeds by an hybrid Monte Carlo algorithm [36] within the publicly available code for QCD with twisted mass fermions [37].

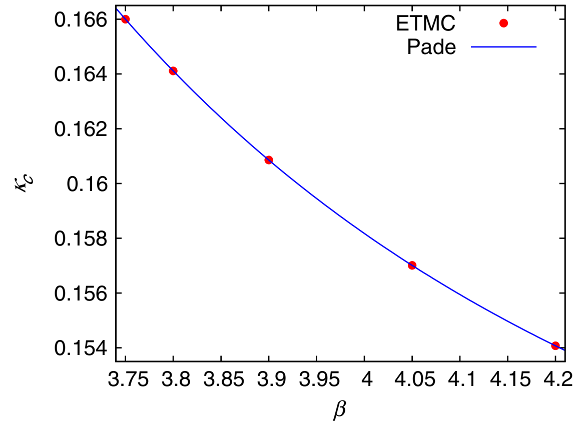

FIG. 1 (color online). Interpolation of the critical hopping parameter from ETMC data.

Wilson fermions are well known to feature unphysical phases for light quarks and coarse lattice spacings. Like the physical parameter space, these get extended to a third direction because of the additional twisted mass parameter in the current formulation. In order to stay away from unphysical regions, knowledge of the bare parameter phase diagram is required, which we have mapped out earlier in a preparatory study [38]. Status reports of our ongoing project have been given at the annual lattice conferences [39,40].

The temperature scale is set by the temporal lattice extent and the lattice spacing, $T = 1/(aN_\tau)$. In order to locate the phase boundary between the hadronic region and the quark gluon plasma, we perform scans in the lattice gauge coupling β, which thus corresponds to a change in temperature of the lattice system. Table I gives the list of runs for different pion masses and the naming scheme that we have adopted for the sake of simplicity. To adjust the masses, ETMC provides parameters for next-to-next-to-leading-order χpt formulas at their values of $\beta \in \{3.8, 3.9, 4.05, 4.2\}$, which can be used to identify the

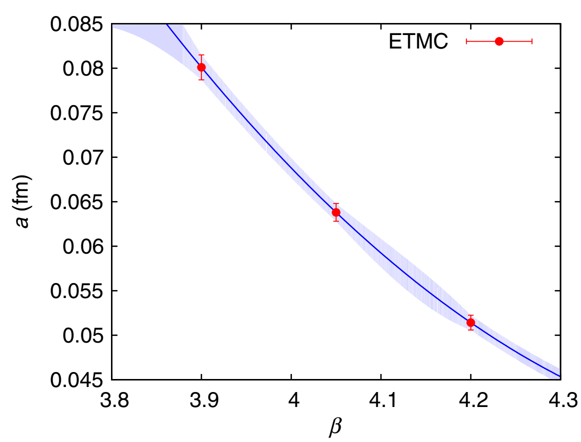

FIG. 2 (color online). Interpolation of the lattice spacing from ETMC data.

TABLE I. List of scans in β. See also Table II.

Run	$N_\sigma^3 \times N_\tau$	RANGE	m_π (MeV)	$r_0 m_\pi$
A12	$32^3 \times 12$	$3.84 \le \beta \le 3.99$	316(16)	0.673(42)
B12	$32^3 \times 12$	$3.86 \le \beta \le 4.35$	398(20)	0.847(53)
C12	$32^3 \times 12$	$3.90 \le \beta \le 4.07$	469(24)	0.998(62)
B10	$32^3 \times 10$	$3.76 \le \beta \le 4.35$	398(20)	0.847(53)

relation $m_\pi(\mu_0)$ at those couplings. For our $N_\tau = 12$ scans, we have relied on the one-loop scaling relation

$$a\mu_0(\beta) = C\exp\left(-\frac{\beta}{12\beta_0}\right), \tag{6}$$

with $\beta_0 = (11 - 2N_f/3)/(4\pi)^2$ and fixing the free parameter C at one of the available couplings. We have found this relation to work sufficiently well to create lines of constant pion mass within the errors quoted in Table I. The run at $N_\tau = 10$ has a constant $a\mu_0 = 0.006$ in the β-interval from 3.865 to 3.930 for which we likewise have the same pion mass within errors in our simulation range. For the other β values, we have adapted the twisted mass according to a two-loop scaling relation similar to the one-loop formula shown above. The free parameter C has been adapted to produce $a\mu_0 = 0.006$ at $\beta = 3.88$.

A final comment concerns the explicit flavor symmetry breaking due to the twisted mass term at finite values of the lattice spacing. This breaking has been investigated by the ETM Collaboration for $T = 0$ theoretically [41] and in simulations [35]. The outcome is that effects from flavor breaking—formally of $O(a^2)$—appear to be negligible in all quantities investigated so far but the neutral pion mass. For this reason we use the charged pion mass throughout the paper. As will be explained in Sec. IV, for our scaling analysis, we need to be close enough to the continuum in order to reproduce chiral symmetry, where flavor breaking should not play any role any longer. Comparison of two lattice spacings appears to justify this assumption. However, a third value of the lattice spacing is required in order to make these statements about the size of lattice artifacts more definite.

III. THERMAL TRANSITION TEMPERATURE

In order to locate the transition, we have used both pure gauge and fermionic observables. The gauge observables are the plaquette

$$P = \frac{1}{6N_c N_\tau N_\sigma^3}\,\mathrm{ReTr}\sum_x \sum_{\mu>\nu} U_{\mu\nu}(x), \tag{7}$$

with

$$U_{\mu\nu}(x) = U_\mu(x)U_\nu(x+\hat{\mu})U_\mu^\dagger(x+\hat{\nu})U_\nu^\dagger(x), \tag{8}$$

and the real part of the Polyakov loop

$$\mathrm{Re}(L) = \frac{1}{N_c}\frac{1}{N_\sigma^3}\,\mathrm{ReTr}\sum_{\mathbf{x}}\prod_{x_4=0}^{N_\tau-1} U_4(\mathbf{x}, x_4). \tag{9}$$

The latter is of particular interest since it is the order parameter of the pure gauge deconfinement transition. Along with these observables, we look at their susceptibilities,

$$\chi_O = N_\sigma^3(\langle O^2\rangle - \langle O\rangle^2). \tag{10}$$

The renormalized (real part of the) Polyakov loop can be determined as [42]

$$\langle \mathrm{Re}(L)\rangle_R = \langle \mathrm{Re}(L)\rangle \exp(V(r_0)/2T), \tag{11}$$

where $V(r_0)$ denotes the static quark-antiquark potential at the distance of the Sommer scale $r = r_0$ [43] to be determined at zero temperature.

The chiral condensate $\langle\bar{\psi}\psi\rangle$ represents the real order parameter of chiral symmetry breaking in the massless limit. An appropriate quantity to locate the chiral phase transition is the chiral susceptibility

$$\chi_\sigma = \frac{\partial\langle\bar{\psi}\psi\rangle}{\partial m_q}. \tag{12}$$

Here, we consider only a part of that expression, the variance per configuration,

$$\sigma^2_{\bar{\psi}\psi} = V/T(\langle(\bar{\psi}\psi)^2\rangle - \langle\bar{\psi}\psi\rangle^2). \tag{13}$$

This quantity shows a peak associated with the chiral transition. Moreover, it is expected to dominate the signal of χ_σ; see, e.g., Ref. [44].

The pion norm

$$|\pi|^2 = \sum_x \left\langle \bar{\psi}(x)\frac{1}{2}\gamma_5\tau^+\psi(x)\bar{\psi}(0)\frac{1}{2}\gamma_5\tau^-\psi(0)\right\rangle \tag{14}$$

is interesting for twisted mass simulations because its definition is independent of the fermion basis. It is connected with the chiral condensate via

$$2m_q|\pi|^2 = -\langle\bar{\psi}\psi\rangle, \tag{15}$$

which has been proven for lattice twisted mass fermions in Ref. [45]. We have used this relation as a check for $\langle\bar{\psi}\psi\rangle$.

At maximal twist the chiral condensate can be renormalized as follows (see the Appendix in Ref. [46] and references cited therein):

$$\langle\bar{\psi}\psi\rangle_R = Z_P\left(\langle\bar{\psi}\psi\rangle + c(g_o)\frac{\mu_0}{a^2}\right). \tag{16}$$

This immediately suggests the form of a subtracted condensate, which is completely standard. However, the subtracted condensate is no longer an order parameter for the chiral transition. It is very easy to fix this problem by adding the zero-temperature chiral condensate in the chiral limit. Thus, we introduce a (re)normalized condensate in terms of the ratio

$$R_{\langle\bar\psi\psi\rangle} = \frac{\langle\bar\psi\psi\rangle(T,\mu_0) - \langle\bar\psi\psi\rangle(0,\mu_0) + \langle\bar\psi\psi\rangle(0,0)}{\langle\bar\psi\psi\rangle(0,0)}, \quad (17)$$

where $\langle\bar\psi\psi\rangle(T,\mu_0)$ means $\langle\bar\psi\psi\rangle$ to be evaluated at nonzero temperature and finite μ_0. $\langle\bar\psi\psi\rangle(0,\mu_0)$ can be obtained from spline interpolations of $T=0$ $\langle\bar\psi\psi\rangle$ data in both the mass μ_0 and β. Additionally, to determine $\langle\bar\psi\psi\rangle(0,0)$ one has to perform a chiral extrapolation of the $T=0$ $\langle\bar\psi\psi\rangle$ data at every β value in which one is interested. We have used a linear extrapolation through three points at every β. The data turned out to be compatible with a linear μ_0 dependence over the whole temperature range we consider here. For the $T=0$ data, we were relying on results provided by the ETM Collaboration.

The fermionic observables have been determined using the technique of noisy estimators, as in Ref. [47]. For $|\pi|^2$ we have calculated ten propagators per gauge configuration on $Z(2)$ noise vectors. $\langle\bar\psi\psi\rangle$ was evaluated using 24 Gaussian volume source vectors for B10, B12, and C12, and 24 $Z(2)$ volume source vectors for A12, respectively. All propagators have been calculated on commodity graphics hardware using NVIDIA's CUDA programming language. The statistics accumulated for the various runs as well as the averages for the Polyakov loop and the chiral condensate are given in Table II.

Quite generally, we find the signals for the transition to be quite smooth and noisy, which presumably is related to the fact that we are merely probing a very soft crossover in our range of pion masses. For a crossover there is no unique definition of a critical temperature as the physics changes smoothly and analytically between the different regions.

TABLE II. Statistics for gauge observables from our simulations as well as expectation values of Re(L) and $\langle\bar\psi\psi\rangle$. Note that the trajectory length differs between the runs. On the apeNEXT (B10, C12 except for $\beta = 4.06$) $\tau = 0.5$, on the HLRN (A12, B12, $\beta = 4.06$ of C12) $\tau = 1$.

β	T [MeV]	STAT	Re(L)	$\langle\bar\psi\psi\rangle$
		A12		
3.8400	187(10)	3471	$6.1(4)\times10^{-4}$	0.0284(1)
3.8600	193(8)	7114	$6.7(3)\times10^{-4}$	0.0264(1)
3.8800	199(6)	3891	$8.8(4)\times10^{-4}$	0.0243(1)
3.9000	205(4)	6666	$9.8(4)\times10^{-4}$	0.0225(2)
3.9300	215(4)	3947	$1.40(4)\times10^{-3}$	0.0199(1)
3.9450	220(4)	4839	$1.60(5)\times10^{-3}$	0.0185(2)
3.9525	222(4)	5962	$1.67(4)\times10^{-3}$	0.0183(2)
3.9600	225(4)	6112	$1.86(5)\times10^{-3}$	0.0176(2)
3.9675	228(4)	7112	$1.98(5)\times10^{-3}$	0.0172(2)
3.9750	230(4)	4505	$2.06(6)\times10^{-3}$	0.0168(2)
3.9900	235(4)	4796	$2.45(5)\times10^{-3}$	0.0158(2)
		B12		
3.8600	193(8)	7198	$5.95(22)\times10^{-4}$	0.03916(12)
3.8800	199(6)	7883	$7.29(22)\times10^{-4}$	0.03677(10)
3.9000	205(4)	9568	$8.67(19)\times10^{-4}$	0.03444(09)
3.9300	215(4)	9204	$1.24(03)\times10^{-3}$	0.03122(13)
3.9500	222(4)	4788	$1.49(05)\times10^{-3}$	0.02932(14)
3.9700	228(4)	8387	$1.96(07)\times10^{-3}$	0.02724(10)
3.9900	235(4)	8968	$2.09(05)\times10^{-3}$	0.02557(13)
3.9950	237(4)	6486	$2.31(04)\times10^{-3}$	0.02515(13)
4.0000	239(4)	6298	$2.51(04)\times10^{-3}$	0.02464(11)
4.0050	241(4)	7353	$2.54(05)\times10^{-3}$	0.02438(10)
4.0100	243(4)	6403	$2.70(05)\times10^{-3}$	0.02391(10)
4.0125	244(4)	10139	$2.81(04)\times10^{-3}$	0.02365(11)
4.0150	245(4)	8950	$2.84(04)\times10^{-3}$	0.02353(10)
4.0175	245(4)	11673	$2.82(03)\times10^{-3}$	0.02346(09)
4.0200	246(4)	10003	$2.88(04)\times10^{-3}$	0.02328(07)
4.0250	248(4)	9878	$3.02(04)\times10^{-3}$	0.02288(10)
4.0300	250(4)	5245	$3.14(05)\times10^{-3}$	0.02251(09)
4.0400	254(4)	5350	$3.43(05)\times10^{-3}$	0.02186(07)
4.0700	266(6)	1024	$4.00(08)\times10^{-3}$	0.02025(10)
4.1000	278(8)	7837	$4.83(09)\times10^{-3}$	0.01894(04)
4.1500	298(10)	4080	$6.17(07)\times10^{-3}$	0.01736(03)
4.2000	320(6)	4160	$7.57(08)\times10^{-3}$	0.01583(02)
4.2500	341(6)	4160	$9.17(07)\times10^{-3}$	0.01451(03)
4.3500	383(8)	4334	$1.21(01)\times10^{-2}$	0.01185(01)
		C12		
3.9000	205(4)	3050	$8.4(5)\times10^{-4}$	0.0465(2)
3.9300	215(4)	3101	$1.16(4)\times10^{-3}$	0.0431(2)
3.9500	222(4)	5822	$1.35(3)\times10^{-3}$	0.0407(2)
3.9700	228(4)	9179	$1.63(3)\times10^{-3}$	0.0379(2)
3.9900	235(4)	5151	$2.11(5)\times10^{-3}$	0.0360(2)
4.0100	242(4)	4640 + 5432	$2.48(5)\times10^{-3}$	0.0341(2)
4.0200	246(4)	5120 + 3324	$2.49(6)\times10^{-3}$	0.0336(3)
4.0300	250(4)	6240 + 3308	$2.92(7)\times10^{-3}$	0.0325(3)
4.0400	254(4)	4080 + 3308	$3.20(7)\times10^{-3}$	0.0315(3)
4.0500	258(5)	4640	$3.57(8)\times10^{-3}$	0.0306(2)
4.0600	262(5)	5523	$3.79(5)\times10^{-3}$	0.0296(1)
4.0700	266(6)	2790	$4.20(5)\times10^{-3}$	0.0288(1)
		B10		
3.7600	200(29)	7760	$1.57(07)\times10^{-3}$	0.05146(10)
3.7800	206(24)	3328	$1.80(10)\times10^{-3}$	0.04769(15)
3.8000	212(20)	3097	$2.25(06)\times10^{-3}$	0.04398(19)
3.8200	218(16)	3516	$2.60(10)\times10^{-3}$	0.04091(17)
3.8400	225(13)	3279	$3.19(08)\times10^{-3}$	0.03783(18)
3.8650	228(11)	3450	$4.80(08)\times10^{-3}$	0.03364(19)
3.8700	234(9)	5900	$4.38(10)\times10^{-3}$	0.03357(14)
3.8750	235(8)	3600	$4.49(10)\times10^{-3}$	0.03351(18)
3.8800	237(7)	8759	$5.07(18)\times10^{-3}$	0.03233(44)
3.8850	239(7)	6400	$4.91(11)\times10^{-3}$	0.03222(40)
3.8900	241(6)	7789	$5.17(13)\times10^{-3}$	0.03258(36)
3.8950	243(6)	4450	$5.52(12)\times10^{-3}$	0.03143(24)
3.9000	244(5)	5973	$5.81(11)\times10^{-3}$	0.03101(20)
3.9100	246(5)	7250	$5.70(12)\times10^{-3}$	0.03085(39)
3.9300	250(5)	8050	$7.23(10)\times10^{-3}$	0.02967(14)
3.9700	258(5)	7276	$8.42(13)\times10^{-3}$	0.02465(07)
4.0500	274(5)	8716	$1.24(2)\times10^{-2}$	0.02060(03)
4.1000	309(5)	1517	$1.44(3)\times10^{-2}$	0.01873(04)
4.2000	333(9)	4131	$2.00(2)\times10^{-2}$	0.01564(01)

A pseudocritical temperature associated with the transition behavior of individual observables is, in general, observable-dependent.

In Figs. 3–6 we show our data for $\sigma^2_{\bar\psi\psi}$ in accordance with Eq. (13) and the susceptibility of the real part of the Polyakov loop [Eq. (9)]. We quite clearly see maxima for $\sigma^2_{\bar\psi\psi}$ in all cases, whereas for the Polyakov loop susceptibility, we find only an onset of certain shoulders for the ensembles A12, B12, and B10. At the higher pion mass case C12, for which we restricted ourselves to smaller statistics, there seems to appear a maximum also for the Polyakov susceptibility.

In order to estimate the pseudocritical β_c for chiral transition, we have modeled the data for $\sigma^2_{\bar\psi\psi}$ with a Gaussian

$$c + a\exp\left(-\frac{(\beta-\beta_c)^2}{\sigma^2}\right). \qquad (18)$$

The results for the corresponding pseudocritical chiral transition temperature T_χ are collected in Table III.

In Fig. 7 we show the renormalized chiral condensate ratio $R_{\langle\bar\psi\psi\rangle}$ and the renormalized Polyakov loop $\langle\mathrm{Re}(L)\rangle$ for the ensembles B12 and B10. The large error bars for the T values in the case of the B10 ensemble reflect the uncertainty in the scale setting.

By determining the inflection point of the renormalized Polyakov loop $\langle\mathrm{Re}(L)\rangle$, we were able to estimate the deconfinement temperatures T_{deconf} for the ensembles B12 and C12, see Table IV.

We cleary see that $T_{\mathrm{deconf}} > T_\chi$ for both higher pion masses. This corresponds to the observation reported in Ref. [42].

From weak coupling analyses (valid at high temperature), it is known that the leading-order a^2 scaling toward the continuum limit might not set in before $N_\tau \gtrsim 16$ [48]. Therefore, discretization effects as a major source of systematical errors need to be thoroughly checked. Since the runs B10 and B12 share a common pion mass and differ only by N_τ, they can be used in order to assess the magnitude of cutoff effects. As can be seen from Fig. 6, the quality of $\sigma^2_{\bar\psi\psi}$ for the B10 ensemble is not yet precise enough to allow for a Gaussian fit. The available data however suggests a maximum at around $\beta \sim 3.82$ that corresponds to a temperature $T \sim 218$ MeV and agrees with T_χ at $N_\tau = 12$. Moreover, the renormalized Polyakov loop and the renormalized chiral condensate (Fig. 7) agree within errors for B10 and B12 indicating small cutoff effects.

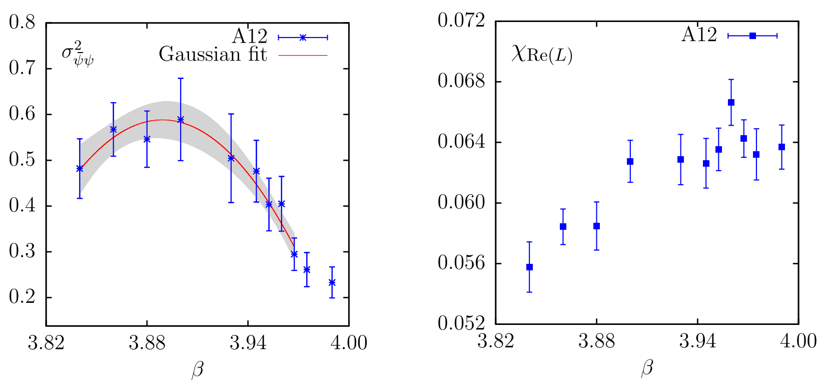

FIG. 3 (color online). $\sigma^2_{\bar\psi\psi}$ (left) and susceptibility of Re(L) (right), both for run A12.

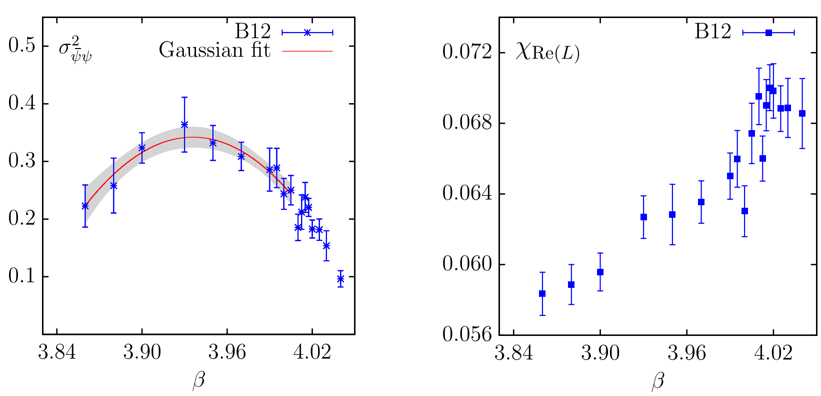

FIG. 4 (color online). $\sigma^2_{\bar\psi\psi}$ (left) and susceptibility of Re(L) (right), both for run B12.

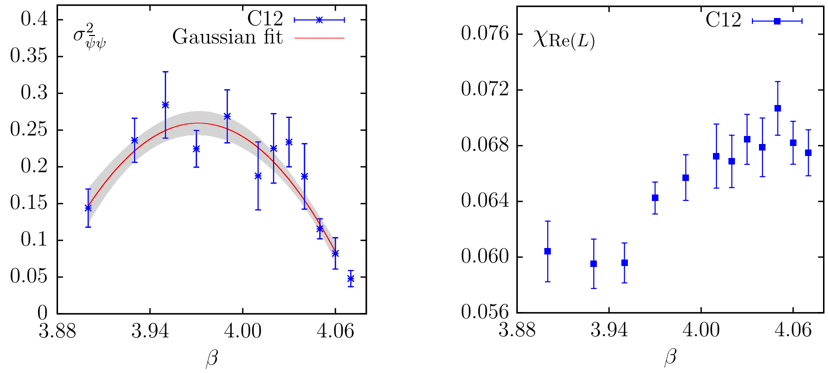

FIG. 5 (color online). $\sigma^2_{\bar\psi\psi}$ (left) and susceptibility of Re(L) (right), both for run C12.

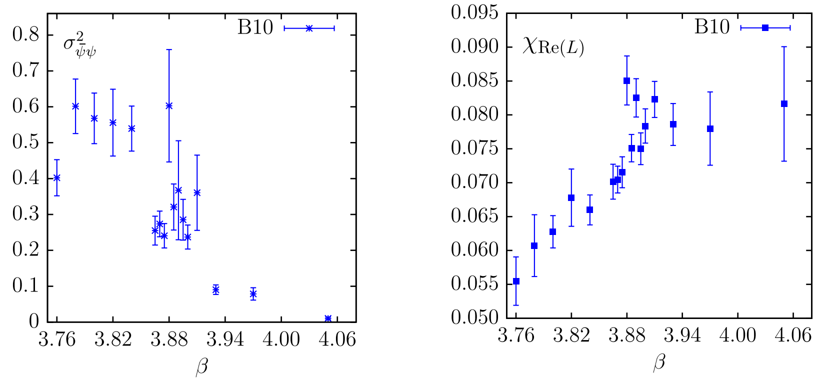

FIG. 6 (color online). $\sigma^2_{\bar\psi\psi}$ (left) and susceptibility of Re(L) (right), both for run B10.

IV. TOWARD THE CHIRAL LIMIT

As indicated in the introduction, the main interest in the $N_f = 2$ thermal transition lies in its chiral limit, for which one would like to unequivocally determine the order of the phase transition. The chiral condensate $\langle\bar\psi\psi\rangle$ then is an order parameter corresponding to the magnetization in an appropriate spin model of the same universality class. Finite quark (and therefore pion) masses break the chiral symmetry explicitly, thus corresponding to an external field. Provided the $N_f = 2$ chiral limit features a second-order transition and belongs to the $O(4)$ universality class, one may extrapolate finite mass simulations using universal scaling relations, which hold within some scaling region around the critical phase transition [19,21]. *A priori* it is not known how far into the massive region scaling extends, i.e., one can merely test consistency of the data with scaling. A further difficulty is that chiral symmetry is broken explicitly for Wilson fermions at finite lattice spacing, even in the massless case. Any universal behavior for these types of fermions thus corresponds to continuum scaling, which can only be observed once discretization errors are sufficiently small. Finally, the scaling relations we employ here are valid in the thermodynamic limit. Dedicated finite-size scaling analyses are required to establish the appropriate lattice sizes, but this is beyond the scope of the present study. Again, we assume our lattices to be sufficiently large and test for consistency with scaling.

TABLE III. List of pseudocritical points for the chiral transition T_χ.

Run	N_τ	β_c	T_χ (MeV)	$r_0 T_\chi$
A12	12	3.89(3)	202(7)	0.437(18)
B12	12	3.93(2)	217(5)	0.473(10)
C12	12	3.97(3)	229(5)	0.500(14)

We begin by attempting a fit of $T_\chi(m_\pi)$ to the scaling form [21,49]

$$T_\chi(m_\pi) = T_\chi(0) + A \cdot m_\pi^{2/(\tilde\beta\delta)}, \tag{19}$$

where we have dressed the critical exponent $\tilde\beta$ with a tilde in order to distinguish it from the lattice coupling. The "external field" in this case is the quark mass specified by the mass parameter $a\mu_0$, which in turn is connected to the pion mass in leading-order (LO) χpt via $m_\pi^2 \sim \mu_0$. Thus, it is important to keep the pion mass small for two reasons: the validity of both the scaling window and the LO of χpt. While there is good reason to expect that our pion masses are sufficiently small for the latter [35], the size of the scaling region remains unknown at present. Unfortunately, we do not have sufficiently many data points or sufficiently small errors in order to determine the exponents but fix the

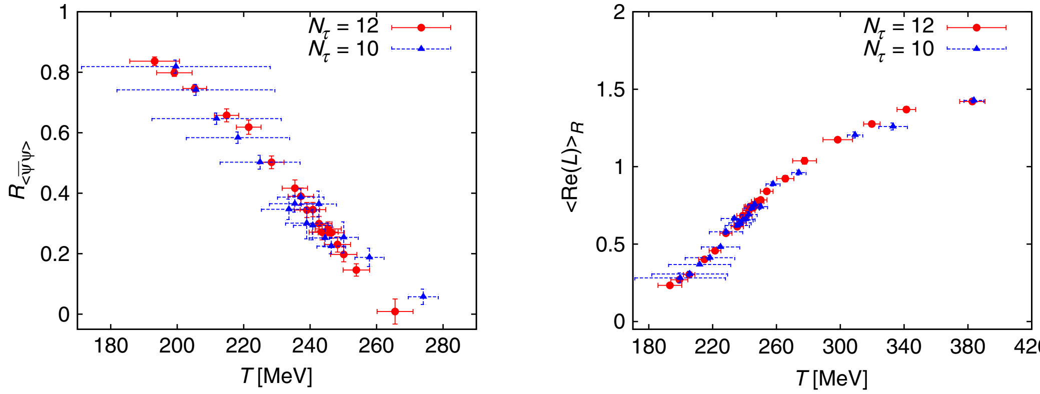

FIG. 7 (color online). Ratio $R_{\langle\bar\psi\psi\rangle}$ according to Eq. (17) (left) and renormalized Polyakov loop $\langle \mathrm{Re}(L)\rangle_R$ (right), both for runs B12 and B10.

exponents and fit A and $T_c(0)$ only. For $O(4)$ we have $2/(\tilde\beta\delta) = 1.08$, and the resulting extrapolation is shown in Fig. 8, giving a chiral critical temperature $T_\chi(m_\pi = 0) = 152(26)\,\mathrm{MeV}$. It is now interesting to ask whether $O(4)$ scaling can be discriminated from other behavior. As discussed earlier, the alternative scenario is a first-order phase transition in the chiral limit. Often in the literature, the same scaling relation is tested by merely changing to "first-order exponents" $(2/(\tilde\beta\delta) = 2)$ [14,50]. Doing so leads to an extrapolation with somewhat larger $T_\chi(m_\pi = 0) = 182(14)\,\mathrm{MeV}$. However, it is unclear to us whether the scaling relation is applicable in this case. First, for a first-order phase transition, there is no diverging correlation length. Approaching T_χ in the infinite-volume limit from above and below proceeds in different phases, with finite correlation length in each. Hence, there is no scaling and no universality in the sense of second-order transitions (in particular, $\tilde\beta = 0$ and $\delta = \infty$ separately). The "critical exponents" usually associated with first-order transitions specify the approach of the thermodynamic limit in finite-size scaling analyses but do not apply to the relation (19) in the thermodynamic limit (for a detailed discussion of scaling for first-order phase transitions, see Ref. [51]). Second, if the chiral limit indeed features a first-order phase transition, it will weaken with finite quark masses until it vanishes in a $Z(2)$ critical endpoint. Figure 9 shows the two possible scenarios. However, this means that coming from the crossover region at larger quark masses, an extrapolation to the chiral limit is never exact, as it would pass through a singularity at the critical point. Rather, the approach of this singularity will again be characterized by scaling, this time in the $Z(2)$ universality class. In this case we may use again the relation (19), but with a finite critical pion mass marking the critical point, $m_\pi^2 \to (m_\pi^2 - m_{\pi,c}^2)$. We have attempted such extrapolations also. Our data are not sufficient to constrain $m_{\pi,c}$. Therefore, Fig. 8 shows two extrapolations, one with $m_{\pi,c} \approx 0$ and another with $m_{\pi,c} \approx 200$ MeV. As the figure illustrates, our extrapolations alone cannot yet discriminate between the first-order and second-order scenarios. This would require drastically smaller pion masses, lower than the physical value even. Nevertheless, using knowledge about T_c from other simulations, we still obtain a tendency. The fit assuming a first-order scenario leads to a critical temperature that is somewhat larger than expected from other investigations [1]. Of course, those extrapolations are likewise valid only in the $O(4)$ scenario; so again this is merely a consistency test.

For a fixed N_τ, assumed to be large enough so as to be sufficiently close to the continuum, it is also possible to obtain the chiral critical β by means of the scaling relation [21,49]

$$\beta_c(h) = \beta_{\mathrm{chiral}} + B \cdot h^{1/(\tilde\beta\delta)}, \qquad h = 2a\mu_0, \quad (20)$$

TABLE IV. List of pseudocritical points for the deconfinement transition T_{deconf}.

Run	N_τ	β_c	T_{deconf} (MeV)	$r_0 T_{\mathrm{deconf}}$
B12	12	4.027(14)	249(5)	0.546(13)
C12	12	4.050(15)	258(5)	0.565(14)

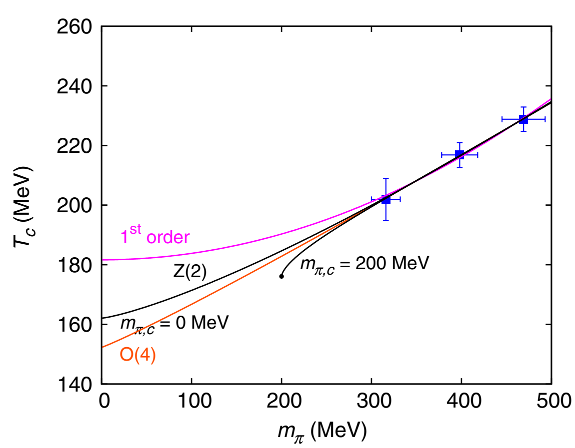

FIG. 8 (color online). Chiral extrapolation for $T_\chi(m_\pi)$ for various scenarios as explained in the text.

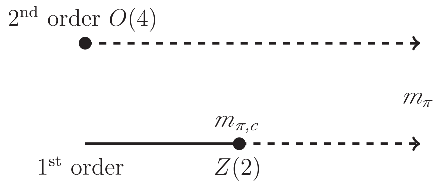

FIG. 9. Illustration of possible scenarios for the $N_f = 2$ chiral limit.

with $1/(\tilde{\beta}\delta) = 0.537$ corresponding to $O(4)$ exponents. For $N_\tau = 12$ our estimates for β_c are shown in Fig. 10 and can be extrapolated in this manner.

Consistent fits have been found taking all three points from A12 to C12 into account. The result for the critical chiral β value is

$$\beta_{\mathrm{chiral}}(N_\tau = 12) = 3.73(9). \tag{21}$$

We have carried out the same fit but with the two lower pion mass values (A12 and B12) only. It ended up with the same value. This result corresponds to $T_\chi(m_\pi = 0) \approx 159(30)$ MeV where the error results from the scale setting. This number is in accord with our fits for $T_\chi(m_\pi)$ for a second-order transition in the chiral limit. Note, however, that the lattice spacing necessary to set the scale stems from an extrapolation to smaller values of β than available from ETMC. This is reflected in the large uncertainty assigned to the temperatures.

Next, the scaling of the magnetic equation of state can be investigated, Fig. 11, in which we follow previous studies [21,24],

$$\langle \bar{\psi}\psi \rangle = h^{1/\delta} c f(d\tau / h^{1/(\tilde{\beta}\delta)}), \tag{22}$$

with

$$\tau = \beta - \beta_{\mathrm{chiral}}. \tag{23}$$

The functional form of the scaling function f for the $O(4)$ case is known [52,53]. Since we do not know the correct normalization for τ and h with respect to QCD, we are

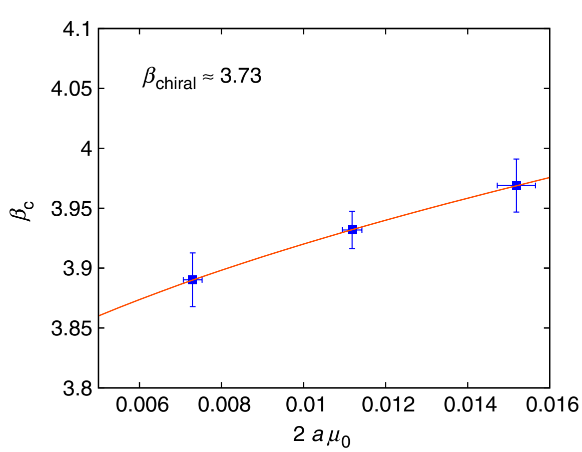

FIG. 10 (color online). Critical couplings β_c as a function of the external field h.

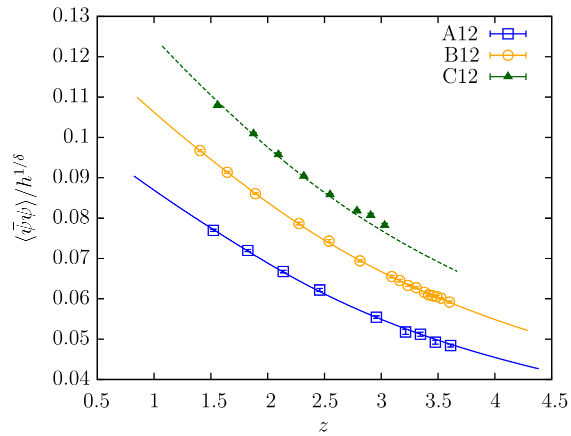

FIG. 11 (color online). Scaling for the bare $\langle \bar{\psi}\psi \rangle$ data at $N_\tau = 12$ as a function of the scaling variable with modelling of scaling violations. The fit shown is for the combined A12 and B12 data (fit number 10 in Table V).

left with two free parameters, c and d, that have to be fitted. We perform the fits in the β intervals from $\beta = 3.83(3.85, 3.89)$ to $\beta = 3.97(4.03, 4.04)$ for A12 (B12, C12), respectively. The fit results are collected in Table V.

A fit for the line A12 works quite well, $\chi^2/\mathrm{dof} = 0.43$, but gives $\beta_{\mathrm{chiral}} = 3.57(4)$, which is smaller than the value estimated above by applying Eq. (20). In general, we observe an increase of χ^2 and a decrease of β_{chiral} with increasing mass. Indeed, B12 yields $\beta_{\mathrm{chiral}} = 3.40(5)$, which would correspond to a much too low critical temperature below 100 MeV, while C12 gives even smaller values with larger χ^2. Thus, the fit seems to account for scaling violations due to large mass by decreasing β_{chiral}.

However, scaling violations due to the quark mass can be taken into account by an ansatz including corrections [24],

$$\langle \bar{\psi}\psi \rangle = h^{1/\delta} c f(d\tau / h^{1/(\tilde{\beta}\delta)}) + a_t \tau h + b_1 h + b_3 h^3 + \cdots \tag{24}$$

We have fitted our data in numerous ways by taking into account one, two, or even three violation terms. Joint fits to the A12 + B12 ensembles are feasible in all three combinations, giving a β_{chiral} the more consistent with the previous determination the more violation terms are included (see Table V). In Fig. 11 we show a combined fit to A12 and B12 fixing $\beta_{\mathrm{chiral}} = 3.73$ from our independent determination with $\chi^2/\mathrm{dof} = 0.63$. Note that these fits with the two lower-order violation terms are not able to include the C12 data with the requirement of a reasonable value of χ^2/dof. However, if we include the next higher violation term $b_3 h^3$ in the combined fit to A12, B12, and C12, we obtain an acceptable $\chi^2/\mathrm{dof} = 1.8$; see the the last line of Table V. We observe that in this case, the fit even prefers a value for β_{chiral} compatible with the one from the analysis based on Eq. (20).

Since we are in a range of the scaling variable $\tau/h^{1/(\tilde{\beta}\delta)}$ where the scaling function is rather flat, judgement on whether there are additional violations of the $O(4)$ behavior

TABLE V. Fit results based on Eq. (24) for several combinations of our data sets and fit parameters. Numbers in bold face have been fixed before fitting. The fit shown in Fig. 11 corresponds to line No. 10.

No	DATA	β_{chiral}	c	d	a_t	b_1	b_3	χ^2/dof
1	A12	3.57(4)	0.14(2)	0.367(7)	**0**	**0**	**0**	0.43
2	B12	3.40(5)	0.22(4)	0.36(2)	**0**	**0**	**0**	0.64
3	C12	3.12(2)	0.42(3)	0.39(2)	**0**	**0**	**0**	2.42
4	A12 + B12	3.368(6)	0.257(6)	0.383(5)	**0**	**0**	**0**	3.31
5	A12 + B12	3.48(2)	0.225(6)	0.48(2)	0.7(1)	**0**	**0**	2.2
6	A12 + B12	3.57(2)	0.152(7)	0.53(2)	**0**	0.90(6)	**0**	1.75
7	A12 + B12	3.82(4)	0.028(9)	1.1(2)	−2.2(2)	2.49(8)	**0**	0.42
8	A12 + B12	**3.73**	0.1279(8)	0.825(8)	4.01(4)	**0**	**0**	76
9	A12 + B12	**3.73**	0.0759(7)	0.81(2)	**0**	1.61(2)	**0**	7.2
10	A12 + B12	**3.73**	0.053(2)	0.74(2)	−1.8(2)	2.23(6)	**0**	0.63
11	A12 + B12 + C12	3.76(2)	0.047(6)	0.83(6)	−1.5(2)	2.20(6)	50(11)	1.8

or not is difficult. Repeating this exercise for the first-order scenario with an endpoint does not give further insight, as the combinations of exponents are very close, $1/(\tilde{\beta}\delta) = 0.537, 0.638$ and $1/\delta = 0.21, 0.20$ for $O(4)$ and $Z(2)$, respectively. Therefore, our data are consistent with the $O(4)$ scenario but do not rule out the possibility of the first-order case. This would require drastically smaller pion masses combined with finite-size studies, as the window for chiral scaling appears to set in for $m_\pi \ll 300$ MeV.

V. CONCLUSIONS

We have presented a (revised) first investigation of the two-flavor thermal QCD transition with maximally twisted mass fermions. Our results are compatible with existing work, although, of course, staggered investigations are much more advanced [12,13,15,54]. The quality of our signals is comparable to recent results with clover improved Wilson fermions [33,50].

For three pion masses in the range 300 MeV $< m_\pi <$ 500 MeV, we have determined pseudocritical temperatures for the crossover from the hadronic regime to the quark gluon plasma. The pseudocritical temperatures—extracted for the two higher mass values—from observables related to chiral and deconfinement transitions, respectively, turned out to be different. Discretization effects in T_c appeared to be small for our lattice spacings, $a < 0.09$ fm.

We have restricted ourselves to pion masses <500 MeV in order to assure the validity of LO χpt as well as the scaling forms in order to extrapolate to the chiral limit. Assuming the scaling forms appropriate for different universality classes, such extrapolations gave critical temperatures in the range $T_c \sim$ 140–200 MeV consistent with other studies. However, detailed fitting analyses demonstrated that the second-order $O(4)$ scaling regime is not yet reached. Scaling violations could be accomodated by leading-order corrections due to finite-mass effects up to $m_\pi \sim 400$ MeV, while heavier masses violate even those corrections. By including higher-order violation effects, reasonable fits could be achieved with β_c values consistent with the other determinations.

We find that truly distinguishing between the different universality classes and thus ruling out a first-order scenario will require much smaller pion masses, $m_\pi \lesssim m_\pi^{\mathrm{phys}}$, as well as finite-size scaling analyses. We hope to address these issues in future investigations.

ACKNOWLEDGMENTS

We express our gratitude to Giancarlo Rossi for clarifying the issue of renormalization in the twisted mass case. Moreover, M. P. L. and L. Z. thank Roberto Frezzotti for useful discussions. O. P. and L. Z. are supported by DFG Grant No. PH 158/3-1 and C. P. by the German BMBF Grant No. 06FY7100. F. B. and M. M. P. acknowledge support by DFG Grants No. GK 1504 and No. SFB/TR 9, respectively. We are grateful to the HLRN supercomputing centers Berlin and Hannover and apeNext in Rome as well as the LOEWE-CSC in Frankfurt for computing resources.

[1] K. Kanaya, Proc. Sci., Lat2010 (2010) 012.
[2] L. Levkova, Proc. Sci., LATTICE2011 (2011) 011.
[3] O. Philipsen, Prog. Part. Nucl. Phys. **70**, 55 (2013).
[4] M. P. Lombardo, Proc. Sci. LATTICE2012 (**2012**) 016.
[5] A. Bazavov *et al.* (HotQCD Collaboration), Phys. Rev. D **86**, 034509 (2012).
[6] A. Bazavov *et al.* (HotQCD Collaboration), Phys. Rev. D **86**, 094503 (2012).

[7] S. Borsányi, Y. Delgado, S. Dürr, Z. Fodor, S. Katz, S. Krieg, T. Lippert, D. Nogradi, and K. Szabó, Phys. Lett. B **713**, 342 (2012).
[8] S. Borsányi, S. Dürr, Z. Fodor, C. Hoelbling, S. Katz, S. Krieg, D. Nogradi, K. Szabó, B. Toth, and N. Trombitas, J. High Energy Phys. 08 (2012) 126.
[9] T. Umeda, S. Aoki, S. Ejiri, T. Hatsuda, K. Kanaya, H. Ohno, and Y. Maezawa (WHOT-QCD Collaboration), Phys. Rev. D **85**, 094508 (2012).
[10] S. Ejiri, K. Kanaya, and T. Umeda (WHOT-QCD Collaboration), Prog. Theor. Exp. Phys. **2012**, 01A104 (2012).
[11] Y. Aoki, G. Endrődi, Z. Fodor, S. Katz, and K. Szabó, Nature (London) **443**, 675 (2006).
[12] S.Borsányi, Z. Fodor, C. Hoelbling, S. D. Katz, S. Krieg, C. Ratti, and K. K. Szabó (Wuppertal-Budapest), J. High Energy Phys. 09 (2010) 073.
[13] S. Borsányi, G. Endrődi, Z. Fodor, A. Jakovác, S. D. Katz, S. Krieg, C. Ratti, and K. K. Szabó, J. High Energy Phys. 11 (2010) 077.
[14] M. Cheng *et al.*, Phys. Rev. D **74**, 054507 (2006).
[15] M. Cheng *et al.*, Phys. Rev. D **81**, 054504 (2010).
[16] A. Bazavov *et al.*, Phys. Rev. D **85**, 054503 (2012).
[17] M. Creutz, Proc. Sci., Confinement8 (2008) 016.
[18] O. Philipsen, Proc. Sci., CPOD2009 (2009) 026.
[19] F. Karsch and E. Laermann, Phys. Rev. D **50**, 6954 (1994).
[20] C. Bernard, T. Blum, C. DeTar, S. Gottlieb, U. M. Heller, J. E. Hetrick, K. Rummukainen, R. Sugar, D. Toussaint, and M. Wingate, Phys. Rev. Lett. **78**, 598 (1997).
[21] Y. Iwasaki, K. Kanaya, S. Kaya, and T. Yoshié, Phys. Rev. Lett. **78**, 179 (1997).
[22] S. Aoki *et al.* (JLQCD), Phys. Rev. D **57**, 3910 (1998).
[23] A. Ali Khan *et al.* (*CP*-PACS), Phys. Rev. D **63**, 034502 (2000).
[24] S. Ejiri, F. Karsch, E. Laermann, C. Miao, S. Mukherjee, P. Petreczky, C. Schmidt, W. Soeldner, and W. Unger, Phys. Rev. D **80**, 094505 (2009).
[25] M. D'Elia, A. Di Giacomo, and C. Pica, Phys. Rev. D **72**, 114510 (2005).
[26] G. Cossu, M. D'Elia, A. Di Giacomo, and C. Pica (2007).
[27] C. Bonati *et al.*, Proc. Sci., Lat2008 (2008) 204.
[28] S. Aoki, H. Fukaya, and Y. Taniguchi, Phys. Rev. D **86**, 114512 (2012).
[29] C. Bonati, P. de Forcrand, M. D'Elia, O. Philipsen, and F. Sanfilippo, Proc. Sci., LATTICE2011 (2011) 189.
[30] R. D. Pisarski and F. Wilczek, Phys. Rev. D **29**, 338 (1984).
[31] A. Shindler, Phys. Rep. **461**, 37 (2008).
[32] T. Umeda, S. Ejiri, S. Aoki, T. Hatsuda, K. Kanaya, Y. Maezawa, and H. Ohno, Phys. Rev. D **79**, 051501 (2009).
[33] V. Bornyakov, R. Horsley, Y. Nakamura, M. Polikarpov, P. Rakow, and G. Schierholz, Proc. Sci., Lat2010 (2011) 170.
[34] B. Brandt, A. Francis, H. Meyer, O. Philipsen, and H. Wittig, Proc. Sci., LATTICE2012 (2012) 073.
[35] R. Baron *et al.* (ETM), J. High Energy Phys. 08 (2010) 097.
[36] C. Urbach, K. Jansen, A. Shindler, and U. Wenger, Comput. Phys. Commun. **174**, 87 (2006).
[37] K. Jansen and C. Urbach, Comput. Phys. Commun. **180**, 2717 (2009).
[38] E.-M. Ilgenfritz, K. Jansen, M. P. Lombardo, M. Müller-Preussker, M. Petschlies, O. Philipsen, and L. Zeidlewicz (tmfT Collaboration), Phys. Rev. D **80**, 094502 (2009).
[39] F. Burger, E.-M. Ilgenfritz, M. Kirchner, M. P. Lombardo, M. Müller-Preussker, O. Philipsen, C. Urbach, and L. Zeidlewicz (tmfT Collaboration), Proc. Sci., Lat2010 (2010) 220.
[40] M. Müller-Preussker, E.-M. Ilgenfritz, K. Jansen, M. P. Lombardo, O. Philipsen, L. Zeidlewicz, M. Kirchner, M. Petschlies, D. Schulze, and C. Urbach (tmfT Collaboration), Proc. Sci., Lat2009 (2009) 266.
[41] P. Dimopoulos, R. Frezzotti, C. Michael, G. C. Rossi, and C. Urbach, Phys. Rev. D **81**, 034509 (2010).
[42] Y. Aoki, Z. Fodor, S. Katz, and K. Szabó, Phys. Lett. B **643**, 46 (2006).
[43] R. Sommer, Nucl. Phys. **B411**, 839 (1994).
[44] C. DeTar, talk at the Kyoto Workshop on Thermal Quantum Field Theory and its Application, 2010.
[45] R. Frezzotti, G. Martinelli, M. Papinutto, and G. Rossi, J. High Energy Phys. 04 (2006) 038.
[46] S. Dinter, V. Drach, R. Frezzotti, G. Herdoiza, K. Jansen, and G. Rossi (ETM Collaboration), J. High Energy Phys. 08 (2012) 037.
[47] P. Boucaud *et al.* (ETM), Comput. Phys. Commun. **179**, 695 (2008).
[48] O. Philipsen and L. Zeidlewicz, Phys. Rev. D **81**, 077501 (2010).
[49] F. Karsch, Phys. Rev. D **49**, 3791 (1994).
[50] V. G. Bornyakov, R. Horsley, S. M. Morozov, Y. Nakamura, M. I. Polikarpov, P. E. L. Rakow, G. Schierholz, and T. Suzuki, Phys. Rev. D **82**, 014504 (2010).
[51] M. E. Fisher and A. N. Berker, Phys. Rev. B **26**, 2507 (1982).
[52] D. Toussaint, Phys. Rev. D **55**, 362 (1997).
[53] J. Engels and T. Mendes, Nucl. Phys. **B572**, 289 (2000).
[54] Y. Aoki, S. Borsányi, S. Dürr, Z. Fodor, S. D. Katz, S. Krieg, and K. Szabó, J. High Energy Phys. 06 (2009) 088.